

Thermal Conductivity of Taylor Phase $\text{Al}_3(\text{Mn},\text{Pd})$ Complex Metallic Alloys*

Denis Stanić,^{a,**} Petar Popčević,^a Igor Smiljanić,^a Željko Bihar,^a Ante Bilušić,^{a,b}
 Ivo Batistić,^c Jovica Ivkov,^a Marc Hegen,^d and Michael Feuerbacher^d

^aLaboratory for the Physics of Transport Phenomena, Institute of Physics, Bijenička c. 46,
 P. O. Box 304, HR-10001 Zagreb, Croatia

^bPhysics Department, Faculty of Natural Sciences and Mathematics, University of Split, Nikole Tesle 12,
 HR-21000 Split, Croatia

^cDepartment of Physics, Faculty of Science, University of Zagreb, Bijenička c. 32, HR-10000 Zagreb, Croatia

^dInstitut für Festkörperforschung, Forschungszentrum Jülich, D-52425 Jülich, Germany

RECEIVED AUGUST 31, 2009; REVISED JANUARY 7, 2010; ACCEPTED JANUARY 12, 2010

Abstract. Thermal conductivity, κ , of Taylor phase $\text{T-Al}_{73}\text{Mn}_{27-x}\text{Pd}_x$ ($x = 0, 2, 4, 6$) complex metallic alloys (CMAs) has been studied in the temperature interval from 2 K to 300 K. The characteristics of κ are typical for the CMAs: a relatively small value, a change of slope at about 50 K and an increase of slope above 100 K. The value of κ is between 2.7 W/m K and 3.7 W/m K at room temperature. The low thermal conductivity has its origin in a complex structure: aperiodic on a short length scale, which leads to frequent electron scattering (*i.e.* to a low electronic contribution to the thermal conductivity), while the large lattice constant defines a small Brillouin zone that enhances *umklapp* scattering of extended phonons. Above 100 K the non-extended (localized) lattice vibrations are thermally excited, and hopping gives a new heat carrying channel resulting in typical increase of the thermal conductivity with temperature.

Keywords: thermal conductivity, Wiedemann-Franz law, Debye model, localized lattice vibrations, bipolar diffusion

INTRODUCTION

Complex metallic alloys (CMAs) denote intermetallic phases whose giant unit cells contain from many tens up to more than a thousand atoms. Inside the giant unit cell the atoms are arranged in clusters with local icosahedral symmetry. Consequently, in CMAs there exist two substantially different physical length scales, so that interesting physical properties may appear. In this paper we study thermal conductivity of the orthorhombic Taylor phase $\text{T-Al}_3(\text{Mn},\text{Pd})$ complex metallic alloys.^{1,2,3} $\text{T-Al}_3(\text{Mn},\text{Pd})$ phase is a ternary solid solution of Pd in the binary $\text{T-Al}_3\text{Mn}$.⁴ Their structure is built of two atomic layers stacked along b crystallographic axis, a flat layer F, and a puckered layer composed of two sublayers P1 and P2. Along this axis, pentagonal columnar clusters are formed.⁵ Therefore, they are considered to be approximants of the decagonal d-Al-Mn

phases. The unit cell of the $\text{T-Al}_3(\text{Mn},\text{Pd})$ phase contains 156 atoms with many of the sites having either fractional occupation or mixed Al/Mn occupation, so that a great inherent chemical disorder exists in the lattice.⁴ Though substitutional site disorder may be expected for the solid solutions $\text{T-Al}_3(\text{Mn},\text{Pd})$, it is not present in the binary $\text{T-Al}_3\text{Mn}$, apart from the ever-present chemical disorder. The aim of this investigation is to uncover the consequences of introducing nonmagnetic Pd admixture in the binary $\text{T-Al}_{73}\text{Mn}_{27}$ on the thermal transport properties. Namely, how the introduction of Pd as a third element in the binary $\text{T-Al}_{73}\text{Mn}_{27}$ alloy influences the thermal conductivity. For the analysis of the thermal conductivity, the results for the spectral conductivity, deduced from the electrical conductivity and thermopower data, were used. In addition, this study complements our previous work^{6–10} of the thermal conductivity of CMAs belonging to different families.

* Presented at the EU Workshop "Frontiers in Complex Metallic Alloys", Zagreb, October 2008.

Dedicated to Professor Boran Leontić on the occasion of his 80th birthday.

** Author to whom correspondence should be addressed. (E-mail: dstanic@ifs.hr, ana@ifs.hr)

EXPERIMENTAL

We studied transport properties (thermal conductivity, electrical conductivity and thermopower) of four polycrystalline samples, members of orthorhombic T-phase AlPdMn with local pentagonal symmetry. The samples were produced from the constituent elements by levitation induction melting in a water-cooled copper crucible under argon atmosphere. All samples have the same structure but different compositions: a binary Al₇₃Mn₂₇ and a ternary Al₇₃Mn_{27-x}Pd_x ($x = 2, 4, 6$). The chemical compositions were determined by powder X-ray diffraction.⁴ Transport properties were investigated on the same specimens and in the same temperature interval from 2 to 300 K. The thermal conductivity κ was measured using an absolute steady-state heat-flow method. The thermal flux through the samples was generated by a 1 k Ω RuO₂ chip-resistor, glued to one end of the sample, while the other end was attached to a copper heat sink. The temperature gradient across the sample was monitored by a chromel-gold differential thermocouple (gold with the fraction of Fe atoms of 0.07 %).¹¹ The electrical resistivity $\rho(T)$ (conductivity $\sigma(T) = 1/\rho(T)$) was measured using the standard four-terminal technique. The thermoelectric power $S(T)$ measurements were performed by applying a differential method with two identical thermocouples (chromel-gold with the fraction of Fe atoms of 0.07 %), attached to the sample with silver paint.¹²

RESULTS AND DISCUSSION

The temperature dependence of the thermal conductivity $\kappa(T)$ for the T-Al₇₃Mn_{27-x}Pd_x ($x = 0, 2, 4, 6$) samples is shown in Figure 1. The $\kappa(T)$ shows a characteristic behaviour for complex metallic alloys (Mg₃₂(Al,Zn)₄₉,¹³ Al₇₄Pd₂₂Mn₄, β -Al₃Mg₂¹⁴ and ϵ -phases (Al-Pd-transition metal)⁸⁻¹⁰ that is: a relatively small value, a change of slope at about 50 K and an increase above 100 K. At room temperature (300 K) the value of κ is in the range 2.7–3.7 W/m K (Table 1). Such a small value of thermal conductivity is a characteristic of thermal insulators like SiO₂¹⁵ and Zr/YO₂¹⁶. A similar small value of thermal conductivity was found also in icosahedral quasicrystals *i*-Al-Pd-Mn^{17,18} and was explained by a small value of the electronic density of states at E_F (small contribution of electrons to thermal conductivity) and no periodicity of sample lattice (small contribution of phonons to thermal conductivity). The T-Al₇₃Mn_{27-x}Pd_x ($x = 0, 2, 4, 6$) samples also show a very low electrical conductivity (Table 1) compared to simple metals. Thus the contribution of electrons, κ_e , to thermal conductivity is much smaller than the lattice (phonon) contribution, κ_l .

Low thermal conductivity, κ , can be explained qualitatively by the influence of structure (disorder) on

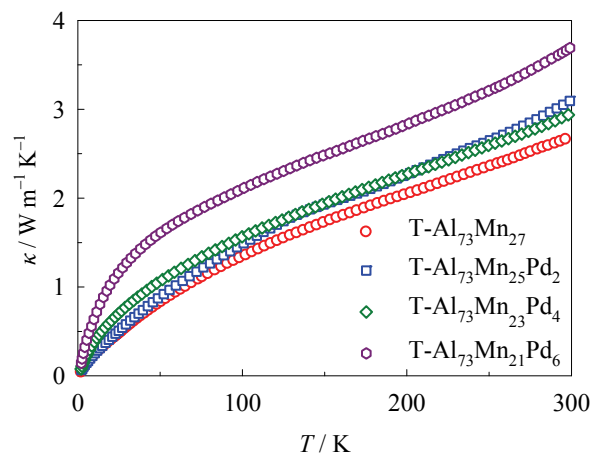


Figure 1. Temperature-dependent thermal conductivity $\kappa(T)$ between 2 and 300 K for samples T-Al₇₃Mn_{27-x}Pd_x ($x = 0, 2, 4, 6$).

Table 1. Room-temperature values of: the electrical, σ , and thermal conductivity, κ , the electronic contribution $L_0T\sigma(T)$ calculated by the WFL, and from the model of spectral conductivity κ_e

Samples	$10^{-4} \sigma$ $\Omega^{-1} \text{m}^{-1}$	κ $\text{W m}^{-1} \text{K}^{-1}$	$L_0T\sigma(T)$	κ_e $\text{W m}^{-1} \text{K}^{-1}$
T-Al ₇₃ Mn ₂₇	1.97	2.69	0.15	0.18
T-Al ₇₃ Mn ₂₅ Pd ₂	2.11	3.09	0.15	0.19
T-Al ₇₃ Mn ₂₃ Pd ₄	13.66	2.95	1.00	1.02
T-Al ₇₃ Mn ₂₁ Pd ₆	19.23	3.70	1.25	1.32

thermal transport of samples studied. The thermal conductivity model appropriate to CMAs with a large-scale periodicity of the lattice and a small-scale atomic clustering structure was described in details in a previous investigation of the *i*-Al-Pd-Mn system.⁶ The electrons and lattice/phonon both contribute to the thermal conductivity $\kappa(T) = \kappa_l(T) + \kappa_e(T)$. It is common practice to estimate the electronic part, κ_e , by using the Wiedemann–Franz law (WFL). The WFL links the electrical conductivity, $\sigma(T)$, and the charge carriers' contribution to the thermal conductivity, $\kappa_e(T)$, of a substance by means of the relationship $\kappa_e(T) = L_0T\sigma(T)$, where $L_0 = 2.44 \times 10^{-8} \text{ W } \Omega \text{ K}^{-2}$ is the Lorenz number. Here we applied a more elaborate analysis based on the Kubo–Greenwood response theory.¹⁹⁻²¹ The Wiedemann Franz law derivation and discussion based on the Kubo–Greenwood formalism can be found in literature.²¹ The central quantity of this formalism is the spectral conductivity function that incorporates both the band structure and the transport properties of the system. All electronic contributions to the transport coefficients, including the electrical conductivity $\sigma(T)$, the thermopower $S(T)$ and the thermal conductivity $\kappa_e(T)$ are related to the spectral conductivity function $\sigma_S(E)$. We have analyzed both the

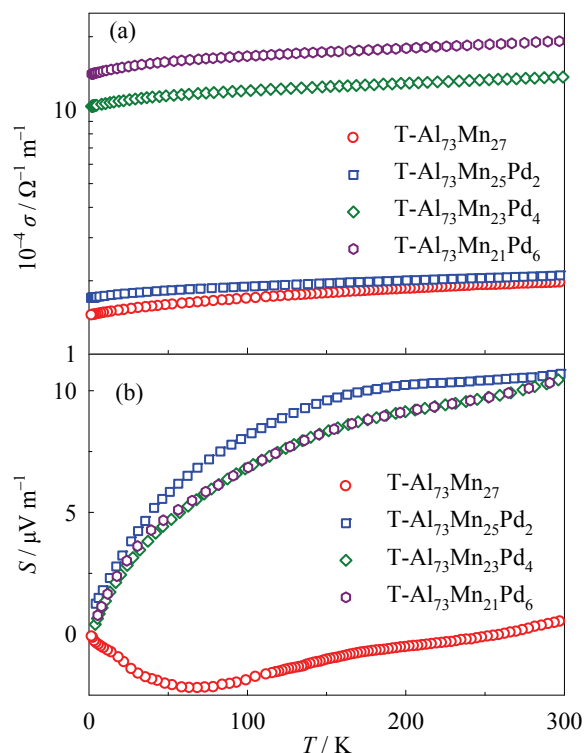


Figure 2. (a) Temperature-dependent electrical conductivity, $\sigma(T)$, and (b) thermopower, $S(T)$, of T-Al₇₃Mn_{27-x}Pd_x ($x = 0, 2, 4, 6$).

electrical conductivity $\sigma(T)$ (Figure 2a), and the thermopower $S(T)$ (Figure 2b) to obtain the properties and the shape of the spectral conductivity function, $\sigma_s(E)$, in the vicinity of the Fermi level. Our final results on the spectral conductivity function are shown in Figure 3. The details of the analysis, that is a modified version of the procedure originally developed by Landau and Macia²²⁻²⁴ and is adjusted to suit the experimental data in this class of compounds, can be found in the literature.²⁵ The most important feature of the spectral function in Figure 3 is the pronounced pseudogap around the Fermi level. Within the energy range of ± 0.1 eV the spectral function loses around 40 percent of its spectral weight. Moreover, our analysis, based on the transport measurements at low temperatures, reveals the fine structure of the pseudogap, featuring the $|E|^{1/2}$ singularity at the Fermi level. Once calculated, the spectral conductivity function can be used to determine the electronic contribution, κ_e , to the thermal conductivity. Results of the electronic contributions calculated from WFL and from the spectral conductivity at room temperature (r.t.) are presented in Table 1. The lattice part, κ_l , is significantly larger than the electronic one, κ_e . That is because the electrical conductivity of these samples is very low, so consequently the electrons also have a small contribution in the heat transport. Although the WFL is inappropriate in the complex metallic alloys,²⁶ the difference

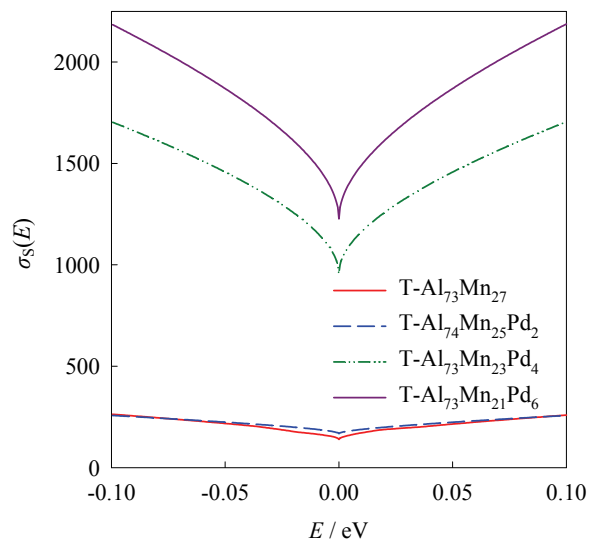


Figure 3. The spectral conductivity function $\sigma_s(E)$ for the T-Al₇₃Mn_{27-x}Pd_x ($x = 0, 2, 4, 6$). The singularity around the Fermi energy (energy scale is shifted so that $E_F = 0$) is clearly pronounced. The sharpness of the pseudogap is directly related to the convex behaviour of the electric conductivity $\sigma(T)$ at low temperatures (see Figure 2a).

between electronic contribution obtained by the spectral conductivity model κ_e and one obtained using WFL is within ten percent. Thus one can use the WFL to predict the electronic contribution to heat transport as a rough approximation.

The lattice contribution, $\kappa_l = \kappa - \kappa_e$, is analyzed considering the propagation of long-wavelength phonons within the Debye model and hopping of localized vibrations. This picture assumes that large atomic clusters of icosahedral symmetry strongly suppress the propagation of phonons in the lattice of complex metallic alloys. Exceptions are long-wavelength acoustic phonons, for which this material is an elastic continuum. In addition to them, the fraction-like localized vibrations within the cluster substructure can participate in the heat transfer via thermally activated hopping. In the simplest model, hopping of localized vibrations is described by the single activation energy E_a , yielding a contribution to the thermal conductivity⁹ $\kappa_H = \kappa_H^0 \exp(-E_a/k_B T)$, where κ_H^0 is a constant. The Debye thermal conductivity is written as:⁶

$$\kappa_D = C_D T^3 \int_0^{\theta_D/T} \tau(x) \frac{x^4 e^x}{(e^x - 1)^2} dx \quad (1)$$

where $C_D = k_B^4 / 2\pi^2 \bar{v} \hbar^3$, \bar{v} is the average sound velocity, θ_D the Debye temperature, τ the phonon relaxation time, $x = \hbar\omega / k_B T$, and $\hbar\omega$ is the phonon energy. The Debye temperature of the investigated T-phases is not known, therefore we have used θ_D value reported for the

related icosahedral *i*-Al–Pd–Mn quasicrystals, were θ_D was commonly found to be close to 500 K.²⁶ Since our $\kappa(T)$ data are available only up to 300 K, it turns out that the fit is insensitive to a slight change of this θ_D value, so a fixed $\theta_D = 500$ K is used. The Debye constant C_D was also not taken as a free parameter, but was instead calculated using $\nu = 4000$ m s⁻¹, a value determined for the *i*-Al–Pd–Mn from the ultrasonic data.

The different phonon-scattering processes are incorporated into the relaxation time $\tau(x)$ and we assume that Matthiessen's rule is valid, $\tau^{-1} = \sum \tau_i^{-1}$, where τ_i^{-1} is a scattering rate related to the *i*-th scattering channel. In analogy to the ϵ -phases in Al–Pd–Mn,⁶ we consider two dominant scattering processes in the investigated temperature interval (from 2 to 300 K). First, the scattering of phonons on structural defects of stacking-fault type with the scattering rate

$$\tau_{\text{sf}}^{-1} = A\omega^2 = \frac{7}{10} \frac{a^2}{\bar{v}} \gamma^2 N_s \omega^2 \quad (2)$$

where a is a lattice parameter, γ is the Grüneisen parameter and N_s is the linear density of stacking faults. The second scattering mechanism are the *umklapp* processes with the phenomenological form of the scattering rate pertinent to complex metallic alloys,¹⁸ $\tau_{\text{um}}^{-1} = B \omega^\alpha T^{4-\alpha}$ and for the total scattering rate we get $\tau^{-1} = \tau_{\text{sf}}^{-1} + \tau_{\text{um}}^{-1}$.

The results of the fitting procedure of the relation $\kappa_1(T) = \kappa_D(T) + \kappa_H(T)$ to the experimental data are shown for T-Al₇₃Mn₂₇ and for T-Al₇₃Mn₂₁Pd₆ in Figure 4a and 4b respectively. The parameters of the fitting procedure, for all investigated samples, are shown in Table 2. From the Figure 4a and 4b, it can be seen that the Debye contribution $\kappa_D(T)$ has a maximum at about 50 K, while it becomes smaller at higher temperatures. A similar behaviour is usual for the periodic structures, where such behaviour originates in the phonon-phonon *umklapp* scattering processes. The parameter A , which describes structural defects of a stacking-fault type, is for all samples close to 10⁷ s⁻¹ K⁻². It is possible to estimate from A the linear density of stacking faults N_s . If we take typical values for the lattice parameter $a \approx 1.5$ nm and the Grüneisen parameter $\gamma \approx 2$, we get N_s of the order of 1 μm^{-1} (Table 2). This micrometer-scale N_s value is comparable to those reported for ψ -Al–Pd–Mn,⁶ *i*-Al–Pd–Mn²⁷ and decagonal d-Al–Mn–Pd.²⁸ Therefore, the stacking-fault-like structural defects also may be considered as the source of phonon scattering at low temperatures in the T-Al₇₃Mn_{27-x}Pd_x ($x = 0, 2, 4, 6$) samples. The parameters B and α define phonon scattering by *umklapp* processes in a phenomenological way. From the fitting procedure we get $\alpha = 1$, so the frequency and temperature dependence of the *umklapp* term is $\tau_{\text{um}}^{-1} \propto \omega^3 T^3$.

Table 2. The fit parameters for the lattice thermal conductivity $\kappa_1 = \kappa_D + \kappa_H$: linear density of the stacking faults N_s , hopping constant κ_{H0} and hopping activation energy E_a

Samples	$N_s / \mu\text{m}^{-1}$	$\kappa_{H0} / \text{W m}^{-1} \text{K}^{-1}$	E_a / meV
T-Al ₇₃ Mn ₂₇	2.0	4.8	17.7
T-Al ₇₃ Mn ₂₅ Pd ₂	2.1	6.8	23.8
T-Al ₇₃ Mn ₂₃ Pd ₄	1.4	2.4	9.4
T-Al ₇₃ Mn ₂₁ Pd ₆	0.6	4.0	11.8

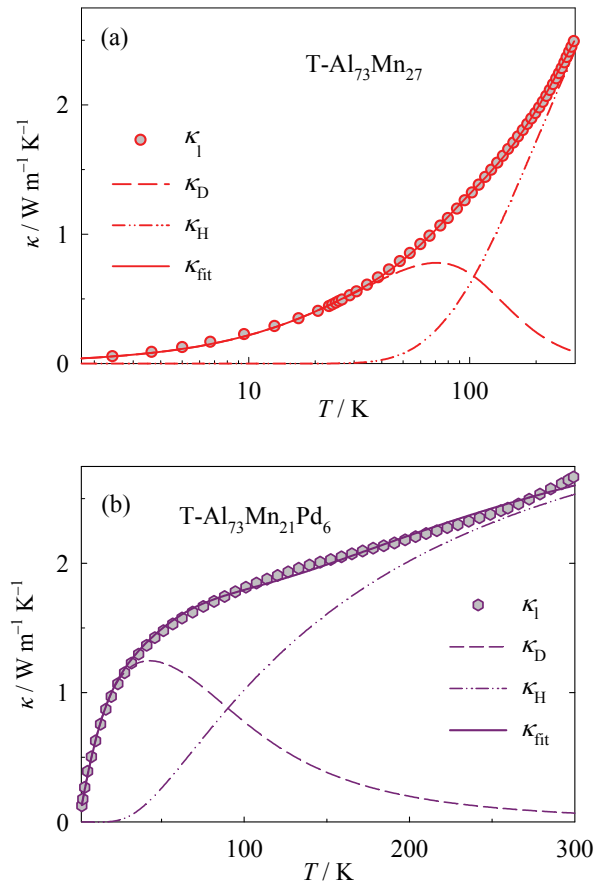


Figure 4. Temperature-dependent lattice thermal conductivity κ_1 together with the Debye contribution κ_D and hopping contribution κ_H of T-Al₇₃Mn₂₇ and T-Al₇₃Mn₂₁Pd₆ shown in log and linear scale (a) and (b) respectively.

The hopping contribution κ_H for all the samples becomes significant above 100 K. The activation energy E_a for all the samples is between 10 and 20 meV and is smaller by factor 2 than the E_a of ψ -Al–Pd–Mn.⁶ This smaller E_a value reflects the considerably less steep increase of $\kappa(T)$ at temperatures above 100 K for our samples, compared to ψ -Al–Pd–Mn. On the other hand, the above values of E_a are in accordance with the inelastic neutron and X-ray⁶ scattering experiments on *i*-Al–Pd–Mn quasicrystals, where dispersionless vibrational

states were identified for energies higher than 12 meV. In quasicrystals such dispersionless states indicate localized vibrations and are considered to be a consequence of a dense distribution of energy gaps in the phonon excitation spectrum. This prevents extended phonons from propagating through the lattice, whereas localized vibrations may still be excited. Therefore, localized vibrations also appear to be present in the giant-unit-cell of T-Al₇₃Mn_{27-x}Pd_x ($x = 0, 2, 4, 6$) samples, where their origin may be attributed to the cluster substructure.

The binary T-Al₇₃Mn₂₇ alloy is stabilized by the introduction of Pd as a ternary substituent element. In the phase diagram, there is a low-temperature phase near the binary T-Al₇₃Mn₂₇, and by introduction of the ternary element the alloy is moved away from that secondary phase and is thus stabilized.⁴ This is apparent from a decrease of the linear density of stacking faults N_s as seen in Table 2. As a consequence of this decrease in the number of the stacking faults, the electrical conductivity is increased (in the case of 6 % of Pd by the factor of even 10) and the thermal conductivity is also increased (see Table 1). The activation energy for the hopping contribution to the thermal conductivity is decreased (except in the case of 2 % of Pd which in general has somewhat uncommon characteristics) but not consistently with the rate of introduction of Pd. The increased number of the stacking faults, hopping activation energy and hopping contribution to the thermal conductivity of the T-Al₇₃Mn₂₅Pd₂ in comparison with the binary and other ternary alloys, mean that transport properties are dominated by the introduction of the chemical disorder rather than the structural stabilization as is the case with other ternary compounds studied here. This is probably the cause of such small (compared to other ternary alloys) increase of the electrical resistivity with respect to the binary alloy. To obtain a better insight into this mechanism of stabilization of the T-phases with the introduction of the ternary element and the influences of the chemical disorder on this process, it is necessary to study ternary T-AlMnPd alloys of composition T-Al₇₃Mn_{27-x}Pd_x with $x < 2$.

CONCLUSION

We have investigated the thermal conductivity of T-Al₇₃Mn_{27-x}Pd_x ($x = 0, 2, 4, 6$) samples which show behaviour in $\kappa(T)$ typical for complex metallic alloys: relatively small values (thermal insulators), a change of slope at about 50 K and an increase of conductivity above 100 K. We have separated $\kappa(T)$ into electron $\kappa_e(T)$ and lattice (phonon) $\kappa_l(T)$ parts which both have small values. The electron part was determined by the spectral conductivity model, and it is much smaller than the lattice one. The reason is a very low electrical conductivity of all the samples which reduces the electron

thermal conductivity. The lattice thermal conductivity is greatly reduced because of enhanced *umklapp* processes of phonon scattering (caused by a large lattice constant and, consequently a small Brillouin zone) and by inherent structural disorder, enhanced also by the introduction of the nonmagnetic Pd admixture in the binary T-Al₇₃Pd₂₇. The introduction of Pd as the ternary element in the binary T-Al₇₃Mn₂₇ alloy has the effect of structural stabilization which is observed from the decrease of the linear density of stacking faults N_s which leads to the reduction of the electrical resistivity and enhanced thermal conductivity. In the case of T-Al₇₃Mn₂₅Pd₂ there is an interplay of chemical disorder introduced with Pd as substituent element and structural stabilization.

Acknowledgements. This work was done within the activities of the 6th Framework EU Network of Excellence "Complex Metallic Alloys" (Contract No. NMP3-CT-2005-500140), and was supported in part by the Ministry of Science, Education and Sports of the Republic of Croatia through the Research Projects: 035-0352826-2848; 035-0352826-2847 and 119-1191458-0512. We are especially grateful to M. Feuerbacher for the provision of the samples and J. Dolinšek for many useful communications. We thank A. Smontara for valuable conversation.

REFERENCES

1. W. Hofmann, *Aluminium* **20** (1938) 865–872.
2. M. A. Taylor, *Acta Metall.* **8** (1960) 256–262.
3. M. A. Taylor, *Acta Cryst.* **14** (1961) 84–84.
4. S. Balanetsky, G. Meisterernst, M. Heggen, and M. Feuerbacher, *Intermetallics* **16** (2008) 71–87.
5. H. Klein, M. Boudard, M. Audier, M. de Boissieu, H. Vincent, L. Beraha, and M. Duneau, *Philos. Mag. Lett.* **75** (1997) 197–208.
6. J. Dolinšek, P. Jeglič, P. J. McGuinness, Z. Jagličić, A. Bilušić, Ž. Bihar, A. Smontara, C. V. Landauro, M. Feuerbacher, B. Grushko, and K. Urban, *Phys. Rev. B* **72** (2005) 064208-1–064208-11.
7. Ž. Bihar, A. Bilušić, J. Lukatela, A. Smontara, P. Jeglič, P. J. McGuinness, J. Dolinšek, Z. Jagličić, J. Janovec, V. Demange, and J. M. Dubois, *J. Alloys Compd.* **407** (2006) 65–73.
8. A. Smontara, I. Smiljanić, A. Bilušić, B. Grushko, S. Balanetsky, Z. Jagličić, S. Vrtnik, and J. Dolinšek, *J. Alloys Compd.* **450** (2008) 92–102.
9. I. Smiljanić, A. Smontara, A. Bilušić, J. Lukatela, D. Stanić, N. Barišić, J. Dolinšek, M. Feuerbacher, and B. Grushko, *Philos. Mag.* **88** (2008) 2155–2162.
10. A. Smontara, A. Bilušić, Ž. Bihar, and I. Smiljanić, *Thermal conductivity of complex metallic alloys*, in: Esther Belin-Ferre (Ed.), *Properties and Application of Complex Metallic Alloys*, World Scientific Publishing (UK) Ltd. England, 2009. pp. 113–147.
11. A. Smontara, K. Biljaković, A. Bilušić, D. Pajić, D. Starešinić, F. Levy, and H. Berger, *Thermal Conductivity of Linear Chain Semiconductor (NbSe₄)₃I*, in: K. E. Wilkes, R. B. Dinwiddie, and R. S. Graves (Eds.), *Thermal Conductivity* **23**, Lancaster: Technomic, 1996. pp. 266–276.
12. A. Smontara, K. Biljaković, J. Mazuer, P. Monceau, and F. Evy, *J. Phys.: Condens. Matter* **4** (1992) 3273–3281.
13. A. Smontara, I. Smiljanić, A. Bilušić, Z. Jagličić, M. Klanjšek, J. Dolinšek, S. Roitsch, and M. Feuerbacher, *J. Alloys Compd.* **430** (2007) 29–38.

14. J. Dolinšek, T. Apih, P. Jeglič, I. Smiljanić, Ž. Bihar, A. Bilušić, A. Smontara, Z. Jagličić, and M. Feuerbacher, *Intermetallics* **15** (2007) 1367–1376.
15. D. M. Zhu, *Phys. Rev. B* **50** (1994) 6053–6056.
16. R. Mevrel, J. C. Laizet, A. Azzopardi, B. Leclercq, M. Poulain, O. Lavigne, and D. Demange, *J. Eur. Cer. Soc.* **24** (2004) 3081–3089.
17. A. Bilušić, Ž. Budrović, A. Smontara, J. Dolinšek, P. C. Canfield, and I. R. Fisher, *J. Alloys Compd.* **342** (2002) 413–415.
18. A. Bilušić, A. Smontara, J. Dolinšek, P. McGuinness, and H. R. Ott, *J. Alloys Compd.* **432** (2007) 1–6.
19. R. Kubo, *J. Phys. Soc. Jpn.* **12** (1957) 570–586.
20. D. A. Greenwood, *Proc. Phys. Soc.* **71** (1958) 585–596.
21. G. V. Chester and A. Thellung, *Proc. Phys. Soc.* **77** (1961) 1005–1013.
22. C. V. Landauro Sáenz, Ph.D. thesis, Fakultät für Naturwissenschaften der Technischen Universität Chemnitz, 2002.
23. C. V. Landauro, E. Maciá, and H. Solbrig, *Phys. Rev. B* **67** (2003) 184206-1–184206-7.
24. E. Maciá, T. Takeuchi, and T. Otagiri, *Phys. Rev. B* **72** (2005) 174208-1–174208-8.
25. Batistić, D. Stanić, E. Tutiš, and A. Smontara, *Croat. Chem. Acta* **83** (2010) 43–47.
26. Ch. Wälti, E. Felder, M. A. Chernikov, H. R. Ott, M. de Boissieu, and C. Janot, *Phys. Rev. B* **57** (1998) 10504–10511.
27. S. Legault, B. Ellman, J. Strom-Olsen, L. Taillefer, T. Lograsso, and D. Delaney, in: S. Takeuchi and T. Fujiwara (Eds.), *Quasicrystals*, Proceedings of the 6th International Conference, World Scientific, Singapore, 1998, p. 475.
28. M. Matsukawa, M. Yoshizawa, K. Noto, Y. Yokoyama, and A. Inoue, *Physica B* **263-264** (1999) 146–148.

SAŽETAK

Toplinska vodljivost Taylorovih faza Al₃(Mn,Pd) kompleksnih metalnih legura

Denis Stanić,^a Petar Popčević,^a Igor Smiljanić,^a Željko Bihar,^a Ante Bilušić,^{a,b}
Ivo Batistić,^c Jovica Ivkov,^a Marc Hegen^d i Michael Feuerbacher^d

^aLaboratorij za fiziku transportnih svojstava, Institut za fiziku, Bijenička c. 46,
P. P. 304, HR-10001 Zagreb, Hrvatska

^bOdjel za fiziku, Prirodoslovno-matematički fakultet, Sveučilište u Splitu, Nikole Tesle 12,
HR-21000 Split, Hrvatska

^cFizički odsjek, Prirodoslovno-matematički fakultet, Sveučilište u Zagrebu, Bijenička c. 32,
HR-10000 Zagreb, Hrvatska

^dInstitut für Festkörperforschung, Forschungszentrum Jülich, D-52425 Jülich, Germany

Prikazani su rezultati ispitivanja toplinske vodljivosti, κ , Taylorovih faza T-Al₇₃Mn_{27-x}Pd_x ($x = 0, 2, 4, 6$) kompleksnih metalnih legura (CMA). Značajka toplinske vodljivosti, κ , u temperaturnom intervalu od 2 do 300 K tipična je za CMA: relativno mali iznos, promjena nagiba krivulje $\kappa(T)$ na oko 50 K i porast vodljivosti iznad 100 K. Iznos toplinske vodljivosti na sobnoj temperaturi je između 2,7 W/m K i 3,7 W/m K. Tako mali iznos toplinske vodljivosti ima porijeklo u kompleksnoj strukturi: aperiodičnost na kratkodosežnoj skali, koja vodi na česta raspršenja elektrona (t.j. na mali doprinos elektrona toplinskoj vodljivosti), dok velika konstanta rešetke definira malu Brillouinovu zonu koja pojačava *umklapp* raspršenje dugovalnih fonona. Iznad 100 K pobuđena su lokalizirana stanja koja mehanizmom preskakivanja (*hopping*) otvaraju novi kanal u vođenju topline i time povećavaju toplinsku vodljivost s porastom temperature.